Journal of High School Science

Cobalt and chlorine co-doped nickel sulfide catalysts: impact of hydrothermal treatment duration on electrochemical activity and stability for ethylene glycol oxidation

Souleyman O[1], Lau J[2]

Submitted: October 2, 2025, Revised: version 1, December 23, 2025, version 2, January 29, 2026, version 3, February 10, 2026
Accepted: February 21, 2026

Abstract

This study investigates the electrochemical activity and stability of cobalt- and chlorine-co-doped nickel sulfide (Co,Cl–NiS) catalysts for ethylene glycol (EG) oxidation in alkaline media. The catalysts were synthesized directly on nickel foam using a one-step hydrothermal method with thiourea, sodium chloride, and cobalt nitrate precursors, with hydrothermal durations of 12, 18, and 24 h. The 12 h catalyst exhibited the highest peak current density (~210 mA cm^{-2}) but showed limited stability (~67.7% retention after 1800 s). In contrast, the 24 h catalyst demonstrated lower activity (~180 mA cm^{-2}) but improved stability (84.1% retention). The 18 h catalyst achieved comparable peak activity (~210 mA cm^{-2}) while exhibiting the highest stability (86.1% retention), indicating an optimal balance between activity and durability. These results reveal a synthesis-duration-dependent activity–stability trade-off, with intermediate hydrothermal treatment producing the most balanced catalytic performance. This work highlights hydrothermal duration as a key parameter for tuning catalytic behavior in dual-doped NiS systems and provides a basis for further structural and mechanistic investigation.

Keywords

Electrocatalysis, Nickel sulfide, Cobalt-doped nickel sulfide, Ethylene glycol oxidation, Alcohol electrooxidation, Hydrothermal synthesis, Nickel foam, Transition metal sulfides, Non-precious metal catalysts, Catalyst stability

[1]Corresponding author: Olivia Souleyman, Hong Kong International School, 1 Red Hill Road Tai Tam, Hong Kong. 260253@hkis.edu.hk

[2]Jaiden Lau, Hong Kong International School, 1 Red Hill Road, Tai Tam, Hong Kong. 270770@hkis.edu.hk

https://doi.org/10.64336/001c.159472

1. Introduction

Electrochemical catalysis plays a central role in sustainable energy conversion, particularly in processes such as water electrolysis and fuel cell reactions. These technologies are critical for clean and renewable energy production, offering alternatives to fossil fuels that significantly contribute to carbon emissions and environmental pollution (1,2). A catalyst is a substance that accelerates a chemical reaction, enabling it to proceed more efficiently. In sustainable energy systems, catalysts facilitate key electrochemical reactions—such as water splitting into hydrogen and oxygen—allowing cleaner energy generation with reduced environmental impact (3).

Nickel sulfide (NiS) is widely studied as a catalyst base material due to its good electrical conductivity, natural abundance, and relatively low cost compared to many transition-metal catalysts. However, NiS has notable limitations, including moderate catalytic activity and limited long-term stability (4). In this work, Co,Cl–NiS was investigated as a strategy to address these challenges by introducing cobalt and chlorine dopants into the NiS lattice. Dual-doping remains comparatively underexplored and may enhance both catalytic activity and structural stability (5).

By examining how cobalt and chlorine co-doping influences NiS performance, this study contributes to the development of improved catalysts for sustainable energy conversion. Although Co,Cl–NiS has received limited attention, this work provides baseline data on the effect of hydrothermal duration in dual-doped NiS systems. These insights can inform future optimization studies, even within the present study's defined scope (6).

2. Materials and Methods

All materials were supplied by The Hong Kong Polytechnic University (PolyU), Hong Kong, China. All reagents were analytical grade and used as received without further purification.

Thiourea (≥99%), sodium chloride (≥99.5%), cobalt nitrate hexahydrate (≥98%), and ethylene glycol (EG) (≥99%, anhydrous) were provided by PolyU. Deionized water (18.2 MΩ·cm) was used as the solvent throughout. Nickel foam (1.6–2.0 mm thickness, ~95% porosity, geometric area 1.0 cm² per sample) was also supplied by PolyU; specific vendor and batch information were not recorded.

Hydrothermal synthesis was performed in a 25 mL PTFE-lined stainless steel autoclave (liner volume ~22 mL) available in-house at PolyU; manufacturer details were not recorded. Hydrothermal treatment was conducted in a Memmert UF55 forced-convection oven (Memmert GmbH + Co. KG, Germany). Electrochemical measurements were performed using a CH Instruments 600E potentiostat (CH Instruments, USA) with an Ag/AgCl (3 M KCl) reference electrode and a platinum mesh counter electrode. The electrolyte for all electrochemical tests consisted of 1.0 M KOH and 1.0 M EG. The potentiostat was calibrated using a standard Ag/AgCl reference solution prior to measurements.

2.1 Pretreatment of nickel foam

Nickel foam (1.6-2.0 mm thickness) was

cleaned to remove surface oxides and contaminants prior to synthesis. Samples were ultrasonicated in acetone for 10 min, followed by ethanol for 10 min. The foam was then rinsed with 30 mL deionized water, etched in 20 mL of 0.5 M HCl for 10 min, and rinsed three times with 30 mL deionized water. Samples were air-dried for 30 min before use. This pretreatment enhanced surface cleanliness and roughness, thereby improving effective electrochemical surface area (4).

2.2 Preparation of precursor solution

Thiourea (0.5 mmol), NaCl (0.01 mmol), and $Co(NO_3)_2 \cdot 6H_2O$ (0.01 mmol) were dissolved in 10 mL deionized water in a standard Griffin beaker. The solution was magnetically stirred at 400 rpm for 30 min to ensure homogeneity. After stirring, the solution was transferred to a 25 mL PTFE-lined stainless steel autoclave. The pretreated nickel foam was immersed in the solution, and the autoclave was sealed (5).

2.3 Hydrothermal treatment

The sealed autoclave containing the precursor solution and nickel foam was placed in the preheated forced-convection oven for hydrothermal synthesis. Hydrothermal durations between 12 and 24 h were initially screened at 2-hour intervals (12, 14, 16, 18, 20, 22, and 24 h). Intermediate durations (14, 16, 20, and 22 h) frequently produced films with weak adhesion or unstable electrochemical responses, likely due to transitional nucleation and growth stages yielding mechanically fragile or structurally heterogeneous layers (7,8). In contrast, 12 h, 24 h, and 18 h treatments consistently yielded uniform, adherent Co,Cl–NiS films with stable electrochemical behavior. These three durations were therefore selected for full electrochemical evaluation (8).

Upon heating, the external stainless-steel body equilibrated first, followed by gradual heat transfer to the internal PTFE liner and solution. The internal solution was estimated to reach near-uniform temperature within approximately 30–45 min (9). Because the autoclave was sealed, heating led to partial water vaporization and increased internal pressure, maintaining liquid-phase conditions > 100 °C.

Although internal pressure was not directly measured, it was approximated based on the saturated water vapor pressure at 120 °C. Accordingly, internal temperature and pressure were assumed to stabilize near the oven setpoint (~120 °C), and pressure values should be interpreted as estimates rather than exact measurements. The elevated temperature and pressure conditions promoted nucleation and growth of the NiS layer in the presence of the cobalt and chlorine precursors (9,10). After completion of the hydrothermal process, the autoclave was removed from the oven and allowed to cool to room temperature (24.0 °C) before opening (11).

2.4 Post-treatment

The nickel foam was removed from the autoclave using tweezers and rinsed thoroughly with deionized water. Samples were rinsed three times with 30 mL deionized water and air-dried at 25 °C for 24 h. Catalyst loading was determined by measuring the mass difference of the nickel foam before and after hydrothermal synthesis using an analytical

balance (±0.01 mg precision, Mettler Toledo ME204, Switzerland). The loading was calculated by dividing the catalyst mass by the geometric electrode area (1.00 cm^2) and reported in mg cm^{-2}.

2.5 Electrochemical analysis

Electrochemical testing was performed in a cylindrical glass cell with a Teflon cap containing electrode ports. The prepared nickel foam (1 cm × 1 cm) served as the working electrode and was connected to the potentiostat via an alligator clip. A platinum mesh served as the counter electrode, and an Ag/AgCl electrode served as the reference electrode. The electrodes were connected to the CH Instruments 600E potentiostat interfaced with CH Instruments software. Linear Sweep Voltammetry (LSV) and chronoamperometry measurements (12) were performed under the parameters summarized in Table 1.

All potentials were converted to the reversible hydrogen electrode (RHE) scale using the standard Ag/AgCl correction. No iR compensation was applied; therefore, all reported currents represent uncorrected values. Current densities were calculated by normalizing measured current to the geometric electrode area (1.00 cm^2). Each experiment was performed in triplicate (n = 3), and results are reported as 95% Confidence Intervals.

Table 1. Linear Sweep Voltammetry parameters.

Parameter	Value	Unit	Notes
Init E	-1	V	Starting potential
Final E	1	V	Ending potential
Scan Rate	0.1	V/s	Sweep speed
Sample Interval	0.001	V	Potential step size
Quiet Time	2	s	Stabilization time before scan
Sensitivity	1e-6	A/V	Current sensitivity
Potential (E)	0	V	Constant E mode
Differential E	0	V	Not active
Sensitivity (Electrode 2)	1e-6	A/V	Same as primary
Mode	Constant E	—	Electrode 2 setting
Swap Electrode 1 and 2 if Scan Rate ≤ 25 V/s	—	—	Unchecked
Auto Sens if Scan Rate ≤ 0.005 V/s	—	—	Unchecked
Open Circuit Potential as Center Potential	—	—	Unchecked
Auxiliary Signal Recording if Scan Rate < 0.1 V/s	—	—	Unchecked

2.6 Data processing and statistical analysis

Each experimental condition was tested in triplicate (n = 3) using independently prepared catalyst samples under identical electrochemical conditions. Current values were extracted from the LSV curves at selected potentials and averaged across the three measurements. The reported uncertainty represents the 95% confidence interval calculated from these replicates rather than point-to-point noise within a single voltammetric scan. Because the same electrode

geometry (1.00 cm² nickel foam) and identical testing conditions were used, variability primarily reflects differences between replicate samples rather than instrumental fluctuations.

Pairwise comparisons (12 h vs 18 h, 18 h vs 24 h, and 12 h vs 24 h) were conducted using an unpaired two-tailed Student's t-test ($\alpha = 0.05$). Statistical analysis was performed on selected current-density values extracted from the LSV curves and on final current density at 1800 s during chronoamperometry. All potentials are reported without iR correction to enable relative performance comparison rather than absolute kinetic evaluation.

2.7 Control experiments

To isolate the effects of cobalt and chlorine co-doping, the following controls were evaluated under identical conditions: [i] bare nickel foam, [ii] undoped NiS, [iii] single-doped Co–NiS and Cl–NiS, and [iv] electrolyte-only control (1.0 M KOH + 1.0 M EG) to account for background current.

3. Results

Figures 1–3 present the LSV curves for the three selected hydrothermal durations: 12 h, 24 h, and 18 h.

3.1 Linear Sweep Voltammetry (LSV) behavior

Figure 1 shows the LSV curve for the catalyst synthesized with 12 h of hydrothermal treatment. The current remains near zero until ~ 0.4 V, indicating an inactive region where ethylene glycol oxidation has not yet begun. ~ 0.4 V, the current begins to increase rapidly, marking the onset potential at which the catalyst becomes electrochemically active. Figure 2 presents the LSV curve for the catalyst synthesized with 24 h of hydrothermal treatment. Similar to Figure 1, the current remains low until ~ 0.4 V, after which a noticeable increase in current is observed as the oxidation reaction begins and catalytic activity increases. Figure 3 shows the LSV curve for the catalyst synthesized with 18 h of hydrothermal treatment. As with the other catalysts, the curve displays a flat inactive region up to ~ 0.4 V followed by a rise in current, indicating activation of the electrochemical oxidation process. Overall, Figures 1–3 show a similar onset potential near ~0.4 V for all samples; however, differences emerge at higher potentials. The 18 h sample exhibits lower current at intermediate potentials (e.g., ~0.6 V) compared to the 12 h sample, but reaches a comparable peak current at 1 V. In contrast, the 24 h sample shows consistently lower current across the full potential range. These differences indicate that hydrothermal duration influences not only activity magnitude but also the rate of current increase after activation.

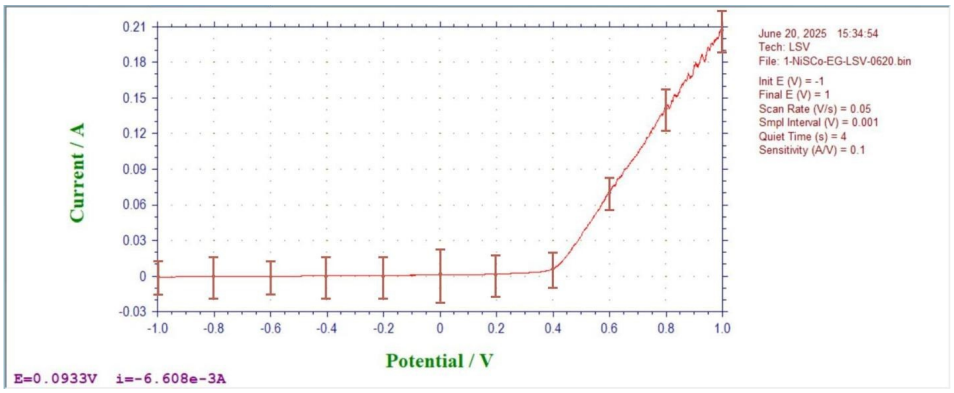

Figure 1. Onset potential (~0.4V) of catalyst synthesized with 12 h hydrothermal treatment.

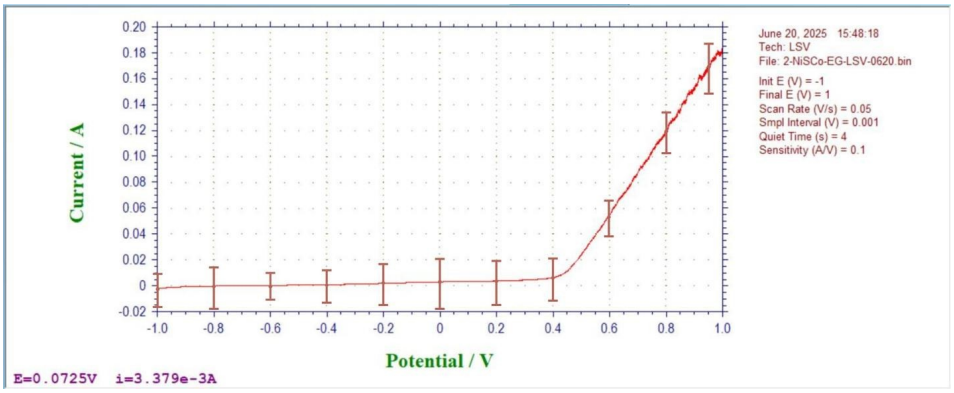

Figure 2. Onset potential (~0.4V) of catalyst synthesized with 24 h hydrothermal treatment.

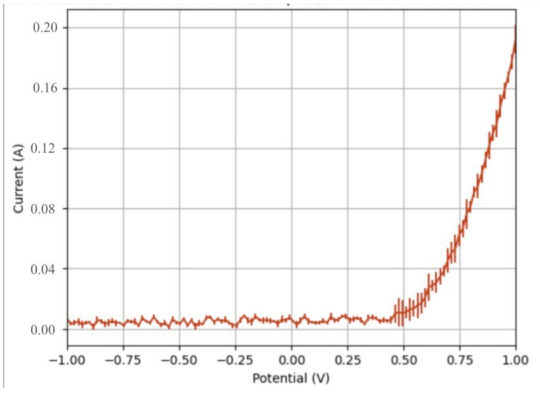

Figure 3. Onset potential (~0.4V) of catalyst synthesized with 18 h hydrothermal treatment.

3.2 Current–time stability trends

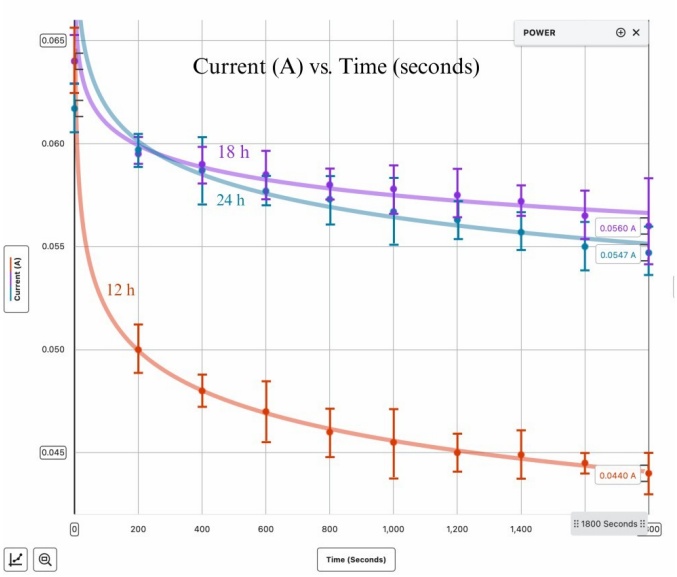

Figure 4. Chronoamperometric stability of Co,Cl–NiS catalysts synthesized with hydrothermal durations of 12 h, 24 h, and 18 h.

Chronoamperometry was conducted for 1800 s at a fixed potential to assess short-term electrochemical stability, with the resulting current–time traces shown in Figure 4. This duration is sufficient to compare relative decay trends but does not represent long-term operational durability. All current values are expressed per geometric area of 1.00 cm^2; therefore 1 A corresponds to 1000 mA cm^{-2} for a 1 cm^2 electrode.

Table 2. Selected current values from the LSV curves shown in Figures 1–3 (Current (A) vs Potential (V))

Potential (V)	0	0.2	0.4	0.6	0.8	1
Average, 12 h	0	0	0.001 ±0.0001	0.075 ±0.004	0.141 ±0.010	0.21 ±0.003
Average, 24 h	0	0	0.004 ±0.0003	0.058 ±0.004	0.12 ±0.009	0.18 ±0.002
Average, 18 h	0	0	0.002 ±0.0001	0.02 ±0.011	0.08 ±0.009	0.21 ±0.003

Control experiments produced only low background currents, with bare nickel foam (~1.2 mA), undoped NiS (~5.1 mA), and single-doped samples (~9–12 mA). These values were substantially lower than those observed for the co-doped catalysts, indicating that simultaneous cobalt and chlorine incorporation enhances electrochemical performance.

All stability data (Table 3) are reported as mean

± 95% confidence interval (n = 3). Individual trial data are not shown for clarity. For comparison of retention behavior, current values were normalized to the mean initial current density of each sample.

Table 3. Summary of chronoamperometric stability performance from Figure 4 (mean ± 95% CI, n = 3)

Hydrothermal duration (h)	Initial current (mA cm^{-2})	Final current at 1800 s (mA cm^{-2})	Retention (%)
12	65.0 ± 3.0	44.0 ± 2.5	67.7 ± 7.4
18	65.0 ± 3.0	56.0 ± 2.5	86.1 ± 5.0
24	65.0 ± 3.0	54.7 ± 2.5	84.1 ± 5.0

Table 4. Catalyst loading and raw mass measurements, replicate measurements (n = 3) are listed as comma-separated values

Hydrothermal Duration (h)	Initial Mass	Final Mass	Δmass (mg)	Loading (mg cm^{-2})
12	52.30,52.10,52.50	54.10,53.88,54.32	1.80,1.78,1.82	1.80,1.80,1.80
18	52.40,52.20,52.60	54.32,54.08,54.50	1.92,1.88,1.90	1.90,1.90,1.90
24	52.30,52.10,52.50	54.30,54.08,54.52	2.00,1.98,2.02	2.00,2.00,2.00

Raw mass measurements and replicate values used to calculate catalyst loading are provided in Table 4. Catalyst loading values were calculated from replicate measurements (n = 3). The uncertainty in Δmass (~±0.014 mg) was estimated by propagation of instrumental error from initial and final mass measurements. The observed variation in Δmass across replicates (~±0.02 mg) is comparable to this instrumental limit, indicating minimal sample-to-sample variation in catalyst loading. While mean loading increases slightly with hydrothermal duration, within-group variation is minimal, and the magnitude of electrochemical differences exceeds that expected from loading differences alone. These values hence suggest that intrinsic catalytic effects dominate over modest variations in loading.

3.3 Effect of hydrothermal duration

Hydrothermal time trades surface quantity for site quality, with 18 h representing an optimal balance between intrinsic activity and surface availability.

The performance differences between the 12 h, 24 h, and 18 h samples exceeded the experimental uncertainty, meaning the improvements were significant within the scope of short- term electrochemical testing. Although small variations may fall within the measurement error, the 18 h sample showed that the differences in current retention during chronoamperometry exceeded experimental uncertainty ($p < 0.05$). Error bars shown in the figures represent 95% confidence intervals calculated from triplicate measurements (n = 3).

These trends are consistent with commonly reported hydrothermal growth behavior of nickel sulfides; however, structural characterization was not performed in this study, and therefore mechanistic interpretations remain speculative (13).

4. Discussion

4.1 Overall trends from screening

Preliminary screening across the 12–24 h hydrothermal range revealed reproducible differences in catalytic activity and short-term stability. Among the tested durations, 18 hours consistently emerged as an intermediate condition, showing markedly improved current retention relative to 12 h while maintaining a high peak current response, although its current at intermediate potentials was lower than that of the 12 h sample. This suggested that key changes influencing electrochemical behavior occurred near this duration, although structural characterization was not performed to directly verify these changes. Durations shorter than 12 h frequently produced films with unstable current responses, whereas extended treatments approaching 24 h showed reduced geometric activity. While sulfur loss or structural densification may occur during prolonged hydrothermal treatment of nickel sulfide systems, these mechanisms were not directly measured here and should therefore be considered speculative. These observations motivated focused electrochemical analysis of the 12 h, 24 h, and 18 h samples.

4.2 Structural interpretation of the 12 h, 24 h, and 18 h catalysts

Hydrothermal treatment can be conceptually viewed as a selective aging process in which less stable surface configurations may gradually reorganize toward more thermodynamically favorable structures. These may include weakly coordinated atoms or highly defective surface motifs that are susceptible to restructuring under alkaline electrochemical conditions. With increasing hydrothermal duration, the density of exposed defect-rich sites may decrease, while the structural stability of the remaining sites may improve.

This trade-off is consistent with the observed decrease in geometric current density alongside improved current retention. Although intrinsic (ECSA-normalized) activity was not quantitatively determined in this study, changes in geometric current density alongside improved stability may indicate differences in intrinsic activity. These interpretations are consistent with general trends reported for hydrothermally synthesized nickel-based sulfides; however, because no direct structural characterization (e.g., XRD, SEM, XPS) was performed in this study, these explanations should be regarded as qualitative rather than definitive.

Within this framework, the 18 h sample appears to represent an intermediate or partial-ordering stage in the hydrothermal growth process. Its behavior combined more moderate initial activity with high structural stability, suggesting that cobalt and chlorine incorporation during synthesis may influence surface stability, although lattice-level incorporation was not directly measured. This intermediate growth state may explain why the

18 h catalyst achieved both improved durability and reasonably high catalytic activity compared to the shorter and longer treatments. With increasing hydrothermal duration, surface roughness and electrochemically active surface area (ECSA) are expected to decrease as the NiS structure becomes more ordered. While this reduces geometric peak current, the remaining active sites are likely more catalytically efficient and stable, implying an increase in intrinsic activity per active site. Hydrothermal time therefore trades surface quantity for site quality, with 18 h representing an optimal balance between intrinsic activity and surface availability. Although geometric current density decreases with increasing hydrothermal duration, the improved stability and reduced defect density suggest that intrinsic activity per active site (i.e., ECSA-normalized activity) likely increases with synthesis time. A qualitative summary of these trends is presented in Table 5.

Table 5. A qualitative summary of these trends illustrating the relative behavior of the 12 h, 24 h, and 18 h catalysts

Metric	12 h	18 h	24 h
ECSA	High	Medium	Low
Geometric peak current	High	High	Lower
Stability	Low	High	Very high
ECSA-normalized activity	Hypothesized lower	Hypothesized intermediate	Hypothesized higher

The trends in Table 5 represent qualitative interpretations based on electrochemical behavior and literature precedent rather than direct structural or ECSA measurements.

Overall, these observations indicate a non-monotonic relationship between hydrothermal duration and electrochemical performance. Moderate hydrothermal treatment stabilizes favorable surface configurations without excessively reducing surface accessibility, whereas prolonged treatment may lead to over-stabilization and diminished activity despite improved durability. The existence of this optimal hydrothermal treatment window highlights how synthesis time alone can govern the balance between catalytic activity and structural stability in Co,Cl co-doped nickel sulfide catalysts.

4.3 Interpretation of Linear Sweep Voltammetry (LSV) results

All three catalysts exhibited onset behavior in the same general potential region, although the 18 h sample showed a slightly delayed rise in current relative to the 12 h and 24 h samples. As a result, no statistically significant difference in onset potential could be concluded across hydrothermal durations. The apparent onset potential was estimated qualitatively as the potential at which current density deviated measurably from the capacitive baseline. Because measurements were performed without iR compensation and at a relatively high scan rate (0.1 V s^{-1}), onset potentials are interpreted qualitatively rather

than as precise kinetic parameters.

Accordingly, variations in catalytic performance are primarily reflected in differences in current magnitude and stability, which are influenced by surface characteristics and dopant incorporation rather than onset behavior.

The 12-hour catalyst produced the highest geometric peak current, which may reflect a higher density of exposed reactive sites associated with shorter hydrothermal treatment, although this was not directly quantified. The 24-hour catalyst produced the lowest geometric peak current, consistent with a possible reduction in accessible surface sites resulting from extended hydrothermal treatment. The 18-hour catalyst again showed high performance, with a peak current density of 210 mA cm^{-2} matching the 12 h (210 mA cm^{-2}) and outperforming the 24 h (180 mA cm^{-2}) samples.

4.4 Analysis of stability tests (current vs time)

According to Table 3, the 18-hour sample exhibited the smallest current decay during the 1800 s chronoamperometric test, indicating the strongest short-term current retention under constant potential. The 24-hour sample also showed high stability, with only slightly greater decay than the 18-hour sample. In contrast, the catalyst synthesized with the shorter hydrothermal duration (12 h) displayed significantly larger current decay over the same time interval. Although no direct post-reaction characterization was performed, the improved stability observed for longer hydrothermal treatments may be consistent with reduced susceptibility to sulfur leaching or surface oxidation; however, these mechanisms remain speculative.

The 12-hour catalyst displayed a sharp decline, falling from ~0.065 A to ~0.044 A by the end of the test. The rapid decay observed for the 12 h sample may be associated with a higher proportion of structurally unstable surface sites, although post-test structural analysis would be required to confirm this mechanism.

The 18-hour sample originated at 65.0 mA cm^{-2} and stabilized at 56.0 mA cm^{-2} after 1800 s, corresponding to an 86.1% retention—higher than the 12-hour sample (~67.7%) and marginally greater than the 24-hour sample (84.1%). These values confirm that substantial improvements in short-term current retention emerge near ~18 hours of hydrothermal treatment.

4.5 Significance of the 18-hour duration

The consistent and balanced behavior of the 18-hour catalyst highlights the importance of this duration in controlling the activity–stability balance in Co,Cl–NiS. The 18-hour condition may correspond to an intermediate growth stage in which sufficient structural stabilization occurs without substantial loss of accessible surface area. While enhanced dopant incorporation is possible, this was not directly verified. This behavior may help explain why improvements in activity and stability do not scale linearly with hydrothermal duration.

For optimization, 18 hours may represent a practical compromise—maintaining high catalytic reactivity while delivering stability similar to fully ordered structures. The

improved retention observed for the co-doped samples suggests that cobalt and chlorine incorporation may influence structural stability; however, systematic comparison of hydrothermal duration effects in undoped systems would be required to confirm this.

4.6 Comparison with existing literature

Previous studies on nickel sulfide catalysts often report that increased crystallinity improves stability but reduces the number of available defect sites for activity. The behavior observed here aligned with these trends but also revealed how cobalt and chlorine co-doping modified them. In particular, few studies identify a distinct intermediate duration where partial crystallinity optimizes both stability and activity. The 18-hour sample therefore represents a meaningful contribution to understanding synthesis–structure–performance relationships in dual-doped sulfide catalysts.

4.7 Alkaline vs acidic EG oxidation

Ethylene glycol oxidation mechanisms differ between alkaline and acidic electrolytes because hydroxyl-assisted pathways dominate in alkaline media, whereas adsorption-controlled pathways are more important in acidic conditions. The present study was conducted exclusively in alkaline electrolyte (1.0 M KOH); therefore, the observations reported here relate specifically to alkaline reaction conditions. Investigation of catalyst behavior in acidic electrolytes remains an important direction for future work.

4.8 Implications within the experimental scope

Adjusting hydrothermal duration provides a controllable synthesis parameter that measurably influences geometric activity and short-term stability under identical electrochemical conditions. Within the scope of the present laboratory-scale measurements, the results show that longer hydrothermal treatment improves short-term stability at the expense of peak geometric current, while intermediate treatment (18 h) offers a balanced activity–stability response. These trends highlight how synthesis time alone can be used as a controllable parameter to compare relative electrochemical behavior under identical testing conditions. The present findings are intended to inform comparative catalyst design strategies rather than to demonstrate readiness for practical, industrial, or large-scale deployment (14). Extended durability testing and application-specific evaluation would be required to assess performance under operational conditions.

4.9 Limitations

This study has several limitations. Hydrothermal durations shorter than 12 hours were not examined because NiS does not fully crystallize below this threshold, while treatments beyond 24 hours risk sulfur loss or structural degradation, restricting the explored time window (15). Only three durations (12, 18, and 24 h) were analyzed in depth, and other synthesis parameters— including temperature, precursor concentration, pH, and dopant ratios —were not systematically varied. As a result, the conclusions isolate time effects but do not capture possible parameter interactions or multidimensional optimization effects.

Electrochemical evaluation was also limited.

Advanced kinetic analyses such as Tafel slope determination, electrochemical impedance spectroscopy (EIS), double-layer capacitance measurements, and turnover frequency estimation were not performed. Consequently, mechanistic interpretation of charge-transfer resistance, reaction kinetics, and active surface area remains incomplete. Because no material characterization was performed, it cannot be conclusively verified that the material is Co,Cl-doped NiS rather than NiS with adsorbed ions.

Structural characterization (XRD, SEM, TEM, XPS, or elemental mapping) was not conducted; therefore, claims regarding crystallinity, defect density, dopant incorporation, and phase evolution remain inferential rather than experimentally verified. In addition, product selectivity and Faradaic efficiency for EG oxidation were not quantified, limiting insight into reaction pathways and catalytic specificity. Long-term durability testing under industrially relevant current densities was also not performed, and scalability, reproducibility across batches, and catalyst–electrolyte compatibility were not evaluated.

4.10 Perspectives

Future work should integrate comprehensive structural and surface characterization to directly correlate hydrothermal duration with crystallographic order, dopant distribution, and defect chemistry. Systematic variation of synthesis parameters beyond time alone would enable multidimensional optimization and clearer structure–property relationships.

Expanded electrochemical analysis—including Tafel slopes, EIS, capacitance measurements, stability testing over extended cycles, and product analysis—would clarify mechanistic pathways and durability limits. Operando or in situ techniques could further reveal dynamic structural changes during catalysis. Finally, scaling studies, electrode engineering, and evaluation under practical device conditions will be essential to determine whether the observed activity–stability balance translates to real-world electrocatalytic systems.

Together, these directions would move the work from baseline performance comparison toward mechanistic understanding and application-ready catalyst design.

5. Conclusion

This study examined the effect of hydrothermal treatment duration on the electrochemical performance of cobalt- and chlorine-co-doped nickel sulfide catalysts for ethylene glycol oxidation. Although durations between 12 and 24 h were screened, only the 12 h, 18 h, and 24 h catalysts produced stable and reproducible films suitable for detailed analysis, and these exhibited clear and systematic differences in activity and stability.

The 12 h catalyst showed the highest initial current density but the lowest stability over 1800 s. In contrast, the 24 h catalyst exhibited lower activity but improved stability. The 18 h catalyst demonstrated a balanced response, maintaining high activity comparable to the 12 h catalyst while achieving the highest current retention. These trends indicate a synthesis-duration-dependent trade-off between activity and stability, with intermediate hydrothermal

treatment providing the most favorable overall performance within the tested conditions.

Catalyst loadings were comparable across all samples (1.80–2.00 mg cm^{-2}) with minimal variation between replicates, indicating that the observed differences in electrochemical behavior primarily reflect intrinsic changes in catalytic properties rather than differences in deposited mass.

Overall, these results show that hydrothermal duration is a key parameter governing the balance between catalytic activity and short-term stability in Co,Cl–NiS systems. However, mechanistic interpretation remains limited by the absence of structural characterization. Future work incorporating techniques such as XRD, SEM, and XPS, along with extended electrochemical testing, will be necessary to establish structure–property relationships and evaluate long-term performance.

Acknowledgement

The completion of this study would not have been possible without the expertise of Professor Ge Jingjie, our mentor and research advisor. We would also like to extend our sincere gratitude to Si Di for the hours she spent assisting us in the lab, and to Fusong Kang for his valuable feedback on this paper.

6. References

1. Zhang, F., Ge, Y., Chu, H., Dong, P., Baines, R., Pei, Y., Ye, M., Shen, J. (2018). Dual-Functional Starfish-like P-Doped Co–Ni–S Nanosheets Supported on Nickel Foams with Enhanced Electrochemical Performance and Excellent Stability for Overall Water Splitting. ACS Applied Materials & Interfaces, 10(8), 7087–7095. https://doi.org/10.1021/acsami.7b18403

2. Ni, Y., Tian, J., Han, Z., Chai, Y., Zhao, C., Wu, G., Li, L. (2025). Catalysis in sustainable energy resources: overview studies of hydrogen, methane, biomass and plastics. Industrial Chemistry & Materials, 3(3), 257–276. https://doi.org/10.1039/d4im00106k

3. Zhang, Y., Fang, J., Wu, Q., Shao, Q., Zhang, T., Jin, Y., et al. (2025). Charge Redistribution in Co-Doped Nickel Sulfide to Accelerate Its Alcohol Electrooxidation. ACS Applied Materials & Interfaces, 17(17), 25410–25418. https://doi.org/10.1021/acsami.5c04673

4. Zhang, J., Balakrishnan, P., Chang, Z., Sun, P., Su, H., Xing, L., Xu, Q. (2022). Boosting the performance of alkaline direct ethanol fuel cell with low-Pd-loading nickel foam electrode via mixed acid-etching. International Journal of Hydrogen Energy, 47(16), 9672–9679. https://doi.org/10.1016/j.ijhydene.2022.01.025

5. Jiang, L., Wei, Z., Ding, Y., Ma, Y., Fu, X., Sun, J., et al. (2022). In-situ synthesis of self-standing cobalt-doped nickel sulfide nanoarray as a recyclable and integrated catalyst for

peroxymonosulfate activation. Applied Catalysis B: Environment and Energy, 307, 121184. https://doi.org/10.1016/j.apcatb.2022.121184

6. Santhosh, N. M., Gupta, S., Vasyl Shvalya, Košiček, M., Janez Zavašnik, Cvelbar, U. (2025). Advancing Oxygen Evolution Catalysis with Dual-Phase Nickel Sulfide Nanostructures. Energy & Fuels, 39(2), 1375–1383. https://doi.org/10.1021/acs.energyfuels.4c05182

7. Chen, Z., Zheng, R., Bao, T., Ma, T., Wei, W., Shen, Y., Ni, B.-J. (2023). Dual-Doped Nickel Sulfide for Electro-Upgrading Polyethylene Terephthalate into Valuable Chemicals and Hydrogen Fuel. Nano-Micro Letters, 15(1), 210. https://doi.org/10.1007/s40820-023-01181-8

8. Zhang, T., Liu, Z., Zhou, S., Jin, L., Zhang, Q., Lin, D., et al. (2024). Construction active sites in nickel sulfide by dual-doping vanadium/cobalt for highly effective oxygen evolution reaction. Journal of Colloid and Interface Science, 655, 167–175. https://doi.org/10.1016/j.jcis.2023.10.161

9. Jin, D., Lee, Y., Kim, I. Y., Lee, C., Kim, M. H. (2023). Impact of controlling the crystallinity on bifunctional electrocatalytic performances toward methanol oxidation and oxygen reduction in binary Pd–Cr solid solution. Journal of Materials Chemistry A, 11(30), 16243–16254. https://doi.org/10.1039/d3ta02782a

10. Lee, M., Kim, S.-I., Lee, M., Ye, B., Kim, T., Kim, H.-D., Lee, J., Lee, D. (2021). Effect of Catalyst Crystallinity on V-Based Selective Catalytic Reduction with Ammonia. Nanomaterials, 11(6), 1452. https://doi.org/10.3390/nano11061452

11. Iago Zapelini, Silva, L., Cardoso, D. (2018). Effect of Hydrothermal Treatment on Structural and Catalytic Properties of [CTA]-MCM-41 Silica. Materials, 11(5), 860. https://doi.org/10.3390/ma11050860

12. Bard, A. J., Faulkner, L. R. *Electrochemical Methods: Fundamentals and Applications*, 2nd ed.; Wiley, 2001.

13. Lemus, J., Bedia, J., Calvo, L., Simakova, I. L., Murzin, D. Y., Etzold, M., et al. (2016). Improved synthesis and hydrothermal stability of Pt/C catalysts based on size-controlled nanoparticles. Catalysis Science & Technology, 6(13), 5196–5206. https://doi.org/10.1039/c6cy00403b

14. Ma, W., Jordi Morales-Vidal, Tian, J., Liu, M.-T., Jin, S., Ren, W., et al. (2025). Encapsulated Co–Ni alloy boosts high-temperature CO_2 electroreduction. Nature, 641(8065),

1156–1161. https://doi.org/10.1038/s41586-025-08978-0

15. Azam Jamsaz, Nhiem Pham-Ngoc, Wang, M., Jeong, D. H., Oh, E.-S., Shin, E. W. (2023). Synergistic effect of macroporosity and crystallinity on catalyst deactivation behavior over macroporous Ni/CexZr1-xO_2–Al_2O_3 for dry reforming of methane. Chemical Engineering Journal, 476, 146821. https://doi.org/10.1016/j.cej.2023.146821